Journal of Zhejiang University-SCIENCE A (Applied Physics & Engineering)
ISSN 1673-565X (Print); ISSN 1862-1775 (Online)
www.jzus.zju.edu.cn; www.springerlink.com
E-mail: jzus@zju.edu.cn

Bearing capacity and failure mechanism of ground improved by deep mixed columns*

Hai-zuo ZHOU[1,2,3], Gang ZHENG[†‡1,2,3], Xiao-xuan YU[1,2], Tian-qi ZHANG[1,2], Jing-jin LIU[1,2]

[1]*School of Civil Engineering, Tianjin University, Tianjin 300072, China*

[2]*Key Laboratory of Coastal Civil Engineering Structure and Safety of Ministry of Education, Tianjin University, Tianjin 300072, China*

[3]*State Key Laboratory of Hydraulic Engineering Simulation and Safety, Tianjin University, Tianjin 300072, China*

[†]E-mail: zhenggang1967@163.com

Received Sept. 26, 2017; Revision accepted Dec. 13, 2017; Crosschecked Mar. 7, 2018

Abstract: Extensive research has investigated the bearing capacity of footings placed on leveled ground improved by deep mixed (DM) columns. However, few studies have focused on the effects of the embedment on the bearing capacity of footings on ground reinforced with DM columns. In geotechnical engineering practice underestimation of the limit load has occurred in China because of the increased use of conventional design methods for reinforced ground with embedment. In this investigation, a numerical model using a rigorous limit analysis tool, known as discontinuity layout optimization (DLO), is established. An equivalent area model is employed with an appropriate stress concentration ratio. Subsequently, a set of design charts of bearing capacity coefficients is produced with a special focus on the bearing capacity coefficient N_q and the failure mechanism. The results show that three failure patterns exist in the composite ground reinforced by DM columns. For cases without embedment, the bearing capacity coefficient N_c increases with the area replacement ratio to a certain value due to the occurrence of general shear failure mechanism. The bearing capacity coefficient N_γ decreases with the area replacement ratio, as the equivalent frictional strength of the reinforced region is reduced. When the embedment is considered, the failure mechanism of composite foundation has a significant influence on the coefficient N_q. Specifically, increase of column length leads to a larger value of N_q when block failure is observed. When a general shear failure pattern occurs, the effect of additional column lengths on the coefficient N_q can be neglected.

Key words: Bearing capacity; Deep mixed (DM) columns; Surcharge; Failure mechanism
https://doi.org/10.1631/jzus.A1700517 **CLC number:** TU4

1 Introduction

Urban structures on soft foundations, such as buildings, slopes, and embankments, impose a great load over large areas, prompting concerns regarding bearing capacity and settlement problems (Duan et al., 2012; Wu et al., 2016). To address these geotechnical issues, a wide range of ground improvement methods have been developed to enhance the bearing capacity and the deformation performance of soft foundations. The deep mixed (DM) technique, which is an economical soil stabilization method, was initially developed in Japan and Sweden in the 1970s (Broms, 1991, 2000) and has been widely used during the past 30 years worldwide (Okumura, 1996; Porbaha, 1998; Bruce, 2001a, 2001b; Cai and Xu, 2002; Tan et al., 2002). The DM method is a technique in which soil is mechanically or hydraulically mixed in situ with a binder, generally based on cement or lime, injected with a pumping system. The soil-cement columns can be produced in the form of slurry (wet mixing) or powder (dry mixing) (Kitazume and Yamamoto, 1998).

‡ Corresponding author

* Project supported by the National Natural Science Foundation of China (Nos. 51378345, 51708405, and 41630641)

ORCID: Hai-zuo ZHOU, https://orcid.org/0000-0002-3346-160X

A series of investigations has been conducted on the bearing capacity characteristics of soft foundations improved by a group of end-bearing DM columns, ranging from theoretical solutions (Bouassida and Porbaha, 2004; Porbaha and Bouassida, 2004; Bouassida et al., 2009), physical models (Kitazume et al., 1999, 2000; Yin and Fang, 2010; Rashid and Safuan, 2011; Dehghanbanadaki et al., 2016), to field tests (Horpibulsuk et al., 2004). The shear failure pattern of DM columns has been addressed when the foundation reaches the limit load. However, few studies have focused on the floating DM columns that are commonly placed in China in ground with thick soft soils. In this situation, the settlement induces more complex failure mechanisms than do end-bearing DM columns. Moreover, ground improved with DM columns is often configured under tall buildings, forming reinforced ground with varying embedment depths, as shown in Fig. 1. Current practice in China involves a design considering the depth modified coefficient equal to 1.0, which ignores the effect of embedment on the increase of bearing capacity of reinforced ground by columns (Zheng et al., 2015). As expected, the bearing capacity of reinforced ground by DM columns is underestimated significantly, in particular for soils with high internal friction angles. The need for an improved bearing capacity analysis is highlighted by the fact that key factors can determine the failure mechanism and bearing capacity of the reinforced ground.

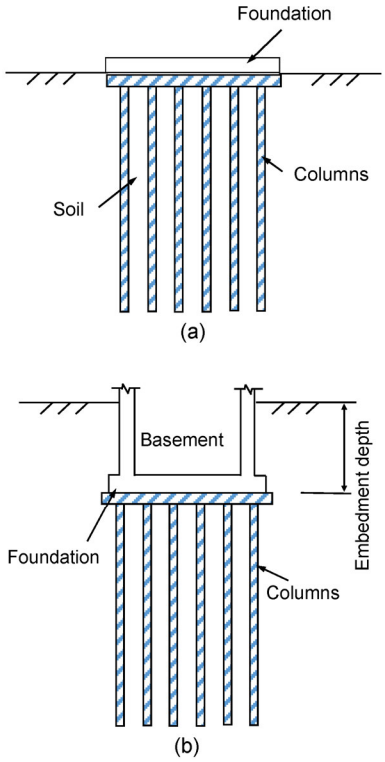

Fig. 1 Schematic of ground reinforced by DM columns without (a) and with (b) embedment

In this study, a discontinuity layout optimization (DLO) technique is used to investigate the bearing capacity of a strip footing on ground improved with a group of floating DM columns. An equivalent area model is adopted, and the accuracy and precision of the current model in evaluating the bearing capacity of DM columns without considering the embedment are verified with the existing physical model and numerical modeling. A set of design charts for bearing capacity coefficients with a wide range of parametric parameters of a group of floating DM columns is presented. Subsequently, the bearing capacity coefficients and the shift of the failure mechanism are discussed.

2 Numerical model

2.1 DLO procedure

The upper bound limit analysis is a strict analytical method for solving complex geotechnical stability and bearing capacity problems without pre-assuming a slip surface. The DLO procedure directly determines the critical layout of discontinuities and the minimum upper bound ultimate load of complex structures (Smith and Gilbert, 2007, 2013). This procedure automatically determines the critical layout of slip lines in a soil mass by discretizing the model, interconnecting the modes with discontinuities, and identifying the critical failure slip by optimization, as shown in Fig. 2. The procedure is analogous to the conventional upper-bound solution that obeys the associated flow rule (Liu et al., 2016). LimitState: GEO (computer software) employs the DLO technique to evaluate critical failure mechanisms and associated upper-bound solutions. This technique provides a highly efficient tool for solving geotechnical problems (Smith and Gilbert, 2007, 2013; Leshchinsky, 2015; Zhou et al., 2018). The reliability and accuracy of this numerical method depend on the node density. Based on a sensitivity analysis, a total number of nodes, which ranges from 2500 to 4000 uniformly distributed across the model, is determined.

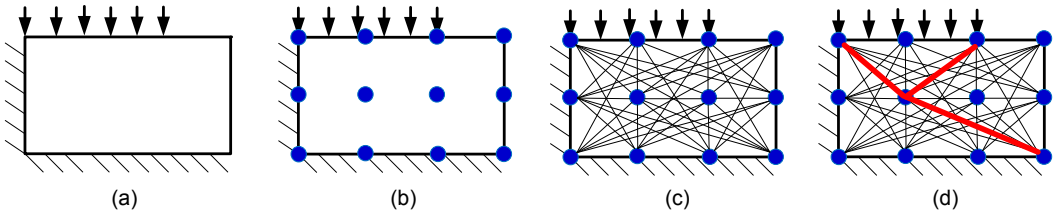

Fig. 2 Procedure of DLO to determine critical collapse mechanism

(a) Starting problem; (b) Discretization of soil by nodes; (c) Interconnection of nodes with potential discontinuities; (d) Identification of critical subset of potential discontinuities by optimization (Smith and Gilbert, 2013)

2.2 Problem definition and equivalent area method

A group of floating DM columns is placed under a strip footing, as shown in Fig. 3a. The strip footing is assumed to be fully rough. Following the classical bearing capacity theory (Terzaghi, 1943), the contribution of the shear strength of the embedment is ignored, and a varying surcharge level q is adopted to study the influence of the embedment depth of foundations on the bearing capacity q_u.

The equivalent area method, which treats the columns and surrounding soil as a composite material, is often adopted in practice to transform the individual column model to a 2D plane strain idealization (Abusharar and Han, 2011; Zhang et al., 2014; Zhou et al., 2017), as shown in Fig. 3b. In the reinforced region, the composite material is replaced by the equivalent homogeneous material. Several methods have been proposed to determine the equivalent properties (Enoki et al., 1991; Priebe 1995; Tan et al., 2008). The most practical method for determining the equivalent properties in the reinforced region is, for simplicity, calculated as the weighted average between the soil and the columns (Aboshi et al., 1979), and can be expressed as follows:

$$c_{eq} = \eta c_c + (1-\eta)c_s, \tag{1}$$

$$\varphi_{eq} = \cot\left[\eta(\tan\varphi_c)\mu_c + (1-\eta)(\tan\varphi_s)\mu_s\right], \tag{2}$$

where

$$\mu_c = \frac{n}{1+(n-1)\eta}, \tag{3}$$

$$\mu_s = \frac{1}{1+(n-1)\eta}, \tag{4}$$

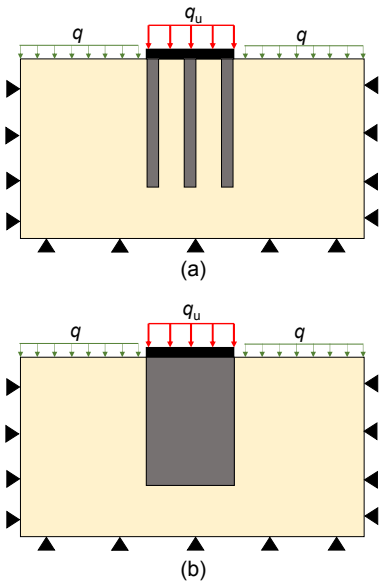

Fig. 3 Schematic of numerical model

(a) Individual column model; (b) Equivalent area model

where η is the area replacement ratio of the stone columns over the soft soil; c_{eq}, c_c, and c_s are the equivalent cohesion, and the cohesion of the column and soil, respectively; φ_{eq}, φ_c, and φ_s are the equivalent friction angle, and the friction angles of the columns and soil, respectively; n is the stress concentration ratio, which is defined as the ratio of the vertical stress on the DM columns to that on the soil.

The combination of the soil and the columns into a composite ground assumes that the effect of columns on the bearing capacity is uniformly distributed throughout the reinforced zone (Sexton et al., 2013), and the equivalent area method ignores the effect of the interaction between columns and soil. This method is commonly used in practice due to its simplicity and its suitability for modeling the performance of floating columns (Sexton et al., 2013). Han (2015) summarized the range of n values for different types of columns. The stress concentration ratio changed continuously during the loading process

Table 1 Comparison between DLO and previous studies on the bearing capacity

No.	η (%)	c_s (kPa)	c_c (kPa)	c_{eq} (kPa)	k_c	q_u (kPa)		Difference (%)
						Previous studies	This study	
1[a]	18.8	11.00	266.50	24.23	59.03	153.20	156.80	2.35
2[a]	18.8	14.10	322.00	22.84	71.99	183.40	193.60	5.56
3[a]	18.8	15.70	292.00	18.60	67.64	188.70	190.10	0.74
4[b]	22	2.66	29.96	8.67	11.26	25.40	26.51	4.37
5[b]	22	2.66	113.29	27.00	42.59	58.30	63.44	8.82
6[c]	26	6.40	83.71	26.50	13.08	77.82	75.22	−3.35
7[c]	26	6.40	87.31	27.44	13.64	79.30	77.11	−2.76
8[c]	26	6.40	87.21	27.41	13.63	54.27	59.67	9.95
9[d]	26	6.20	89.62	27.89	14.45	52.33	59.98	14.62
10[d]	26	6.40	83.71	26.50	13.08	77.82	90.11	15.79
11[e]	13.1	9.5	85.8	19.50	9.03	71.60	70.84	1.07
12[e]	19.6	10.3	88.3	25.59	8.57	85.00	86.33	−1.54
13[e]	26.2	9.7	82.8	28.85	8.54	94.00	91.12	3.16

[a] Data from model tests of Bouassida and Porbaha (2004); [b] Data from model tests of Omine et al. (1999); [c] Data from numerical simulation of Rashid et al. (2017); [d] Data from model tests of Rashid et al. (2015); [e] Data from model tests of Dehghanbanadaki et al. (2016). k_c: relative cohesion ratio of the column to the soft soil

(Juran and Guermazi, 1988) and dropped to a low value when failure was reached (Fattah et al., 2011; Zhang et al., 2014; Zhou et al., 2018). Therefore, a stress concentration ratio n=2.0 is selected in this study.

2.3 Validation

Before being used to generate the design charts of bearing capacity coefficients, the equivalent area model was first validated with the individual column model. Fig. 4 shows a comparison between the individual column model and the equivalent area model in terms of the bearing capacity q_u versus friction angles for an area replacement ratio η varying from 20% to 40%. The results obtained by the equivalent area model were slightly larger than those of the individual column model for low friction angles, whereas that behavior was reversed when the friction angle φ values were increased. Generally, the equivalent area model coincided with the individual column model.

For further calibration of the DLO procedure, the predicted bearing capacity obtained by DLO was compared with that of several laboratory tests (Omine et al., 1999; Bouassida and Porbaha, 2004; Rashid et al., 2015; Dehghanbanadaki et al., 2016) and a numerical model (Rashid et al., 2017) for varying affecting parameters, as shown in Table 1. Those investigations were conducted under a rigid footing,

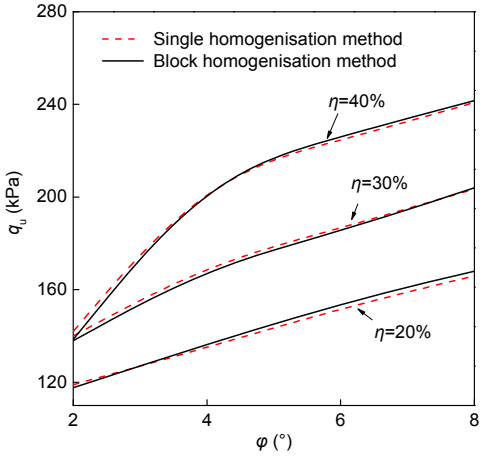

Fig. 4 Comparison between the individual column model and equivalent area model

and all tests were performed under undrained conditions. All discrepancies between DLO and the solutions obtained previously were within 16%, demonstrating the accuracy and precision of the present numerical simulation.

3 Results

The failure pattern of composite ground reinforced by DM columns was first investigated in terms of the individual column model and the equivalent

area model, as shown in Fig. 5. Three types of failure patterns can be categorized: general shear failure, local shear failure, and block failure, which are coincident with the findings from research on stone columns (Hanna et al., 2013). For the general shear failure mechanism, the DM columns experienced shear failure, in which the failure slip passed both soil and columns. A wedge was formed within the reinforced region without significant deformation. This mechanism coincides with that observed in previous studies on end-bearing DM columns (Yin and Fang, 2010; Dehghanbanadaki et al., 2016). When local shear failure occurred, the DM columns penetrated the soil, and a rigid wedge formed simultaneously within the reinforced zone. For the block failure mechanism, no clear rigid cone was observed. The DM columns together with the soil were punched into the soil at the base of the columns. In this failure type, the resistance at the base of the columns and the shear strength of the soil along the length of the exterior columns contributed to the bearing capacity. The predictions of the individual columns model and the equivalent area model were similar, which further demonstrates the accuracy of the equivalent area method.

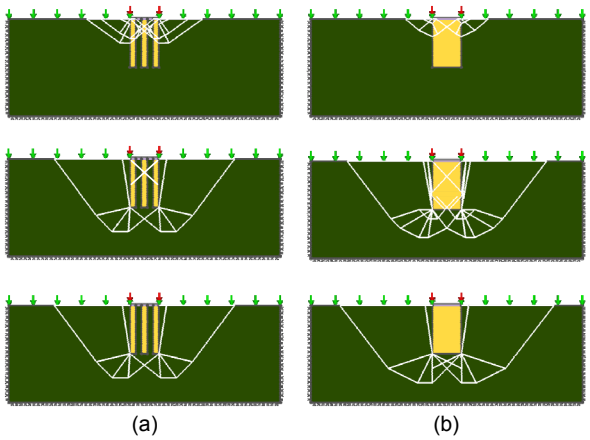

Fig. 5 Failure mechanism of composite ground reinforced by DM columns: (a) individual column model; (b) equivalent area model

Previous investigation of the bearing capacity issue mainly investigated purely cohesionless and purely cohesive soils. Leshchinsky (2015) emphasized the need to address bearing capacity by consideration of both cohesive and frictional aspects, which are common for native soils. He adopted DLO procedure with effective stress analysis to investigate the bearing capacity of strip footings on *c*-*φ* soils. An extended study focusing on the failure mechanism can be found in (Zhou et al., 2018), and an analogous analysis for *c*-*φ* soils was performed in that study. Moreover, a linearly elastic perfectly plastic model with the Mohr-Coulomb failure criterion was adopted in the numerical model. In practice, the strength of DM columns is determined by unconfined compressive strength tests. Given the inconclusive investigation in respect of permeability and engineering conservation, the shear strength of soil-cement was considered in previous studies for both stability and settlement problems (Huang and Han, 2009; Ye et al., 2013; Chai et al., 2015, 2017). The shear strength of the DM columns was considered as 200 kPa (Yapage et al., 2014). In addition, the effect of modulus and Poisson's ratio is negligible for the bearing capacity issue (Zhou et al., 2017). A dimensionless parameter of column length L/B is defined as the ratio of length of the DM columns to the width of the footing. In practice, a square or triangular grid of columns is often used, which offers an area replacement ratio, η, between 10% and 50% (Karstunen, 1999; Kitazume and Terashi, 2002). Thus, various area replacement ratios from 10% to 40% were adopted. Following classical bearing capacity theory and previous study (Zhou et al., 2017), the contribution of the soil shear strength of soil within embedment was neglected, and surcharge levels of 20–60 kPa were adopted in the model. The weight of columns was assumed as that of the soil for simplicity (Huang and Han, 2009; Zhang et al., 2014). The interface between DM columns and soils was assumed to form a perfect bond in DLO, and this behavior has been verified through numerical modelling (Bouassida et al., 2009; Rashid et al., 2017). Table 2 presents the design scenarios estimated by the DLO procedure.

To present the design charts of a group of floating DM columns, the superposition method suggested by Terzaghi (1943) was employed to calculate the bearing capacity coefficients as follows:

$$q_{\mathrm{u}} = c_{\mathrm{s}} N_{\mathrm{c}} + q N_{\mathrm{q}} + \frac{1}{2}\gamma_{\mathrm{s}} B N_{\gamma}, \tag{5}$$

where the bearing capacity factors N_c, N_q, and N_γ represent the effects of the soil cohesion c_s, surcharge level q, and unit weight of the soil γ_s, respectively.

Fig. 6 shows the bearing capacity charts of coefficient N_c versus the area replacement ratio η at various column lengths L/B. It can be seen that the N_c value increases with the area replacement ratio η until this parameter reaches a certain threshold value. This value is influenced by the column length L/B. Specifically, the inflection point increases when the column length is large. For a relative high friction angle (e.g. φ=10°) reinforced with long columns (e.g. L/B=4), the N_c value shows a linearly increasing trend with increasing area replacement ratio η. Generally, the peak N_c value increases with increasing column length L/B.

Table 2 Parameters in the bearing capacity analysis

Parameter	Value
Soil cohesion, c_s (kPa)	10
Friction angles of soil, φ_s (°)	2, 6, 10
Unit weight of soil, γ_s (kN/m^3)	18
Length of DM columns, L/B	2, 3, 4
Shear strength of DM columns, c_c (kPa)	200
Unit weight of DM columns, γ_c (kN/m^3)	18
Area replacement ratio, η (%)	10, 20, 30, 40
Surcharge level, q (kPa)	20, 40, 60

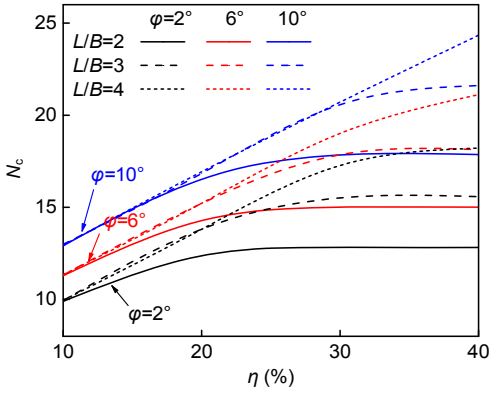

Fig. 6 Bearing capacity charts for coefficient N_c

Fig. 7 presents the bearing capacity charts of coefficient N_γ versus the area replacement ratio η at various column lengths L/B. For friction angles φ=6° and 10°, N_γ exhibits a gentle reduction with increasing area replacement ratio η. In those cases, a general shear failure mechanism occurs. This is because the increase of area replacement ratio reduces the equivalent friction angle in the reinforced zone, leading to a decrease of the coefficient N_γ. Notably, an increasing trend appears for η for the short columns in the soils with low friction angles (i.e. L/B=2 and φ=2°; L/B=3 and φ=2°).

To clearly show the influence of affecting factors on the N_q value, the bearing capacity charts of coefficient N_q are plotted versus the column length L/B at various values of area replacement ratio η and surcharge level q, as illustrated in Fig. 8. Three different trends of N_q with increasing column length can be observed. To be specific, for high η and low φ values (e.g. η=40° in Fig. 8a), the coefficient N_q increases with column length L/B. For relatively high-friction soils improved by DM columns with low area replacement ratio (e.g. η=20° in Fig. 8c), the coefficient N_q is insensitive to the column length. Otherwise, the N_q values decrease with increasing column length, but the increase ratios are inconsistent. This phenomenon is mainly because of the transition of the failure mechanism. N_q will be discussed together with coefficients N_c and N_γ in the following sections.

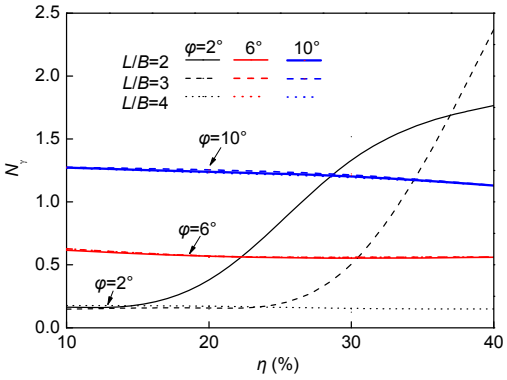

Fig. 7 Bearing capacity charts for coefficient N_γ

4 Discussion

In this section, the phenomenon of the design charts with different bearing capacity coefficients is elaborated. Fig. 9 shows the schematic of coefficient N_c with η, with the corresponding failure mechanism

incorporated. The N_c value uniformly increases with increasing η until a threshold value is reached. The starting point represents a general shear failure pattern, and the N_c value increases with η because of the contribution of a higher shear strength in the reinforced region. As η increases, the increase ratio of N_c decreases, indicating that the mechanism changes to a local shear failure pattern. Once η exceeds a threshold value, a block failure mechanism occurs in which the influence of shear strength in the reinforced region on the bearing capacity can be neglected. This finding is different from the results of Hanna et al. (2013) studying the performance of stone columns installed in clay under rigid foundations. As shown in Fig. 6, the curve increases linearly without an inflection point (i.e. φ=10° and L/B=4) because there is no transition of the failure mechanism.

Similarly, due to the occurrence of a general shear failure pattern, a gentle reduction is observed in Fig. 7. A counterintuitive trend of initial reduction and consequent increase of coefficient N_γ is presented in Fig. 10 with the corresponding failure mechanism. For cases of low frictional strength soil improved by short columns, a general shear failure pattern arises for a low area replacement ratio. As the area replacement ratio initially increases, the equivalent friction angle in the reinforced region and N_γ are reduced because N_γ is relatively sensitive to the friction angle. Subsequently, the curves increase with the increasing area replacement ratio. In this stage, a local shear failure pattern arises in which the frictional strength within the reinforced region and at the base of the columns each contributes to the coefficient N_γ. Then, a block failure pattern arises when the area replacement ratio is large, leading to a decreased influence of the area replacement ratio on N_γ.

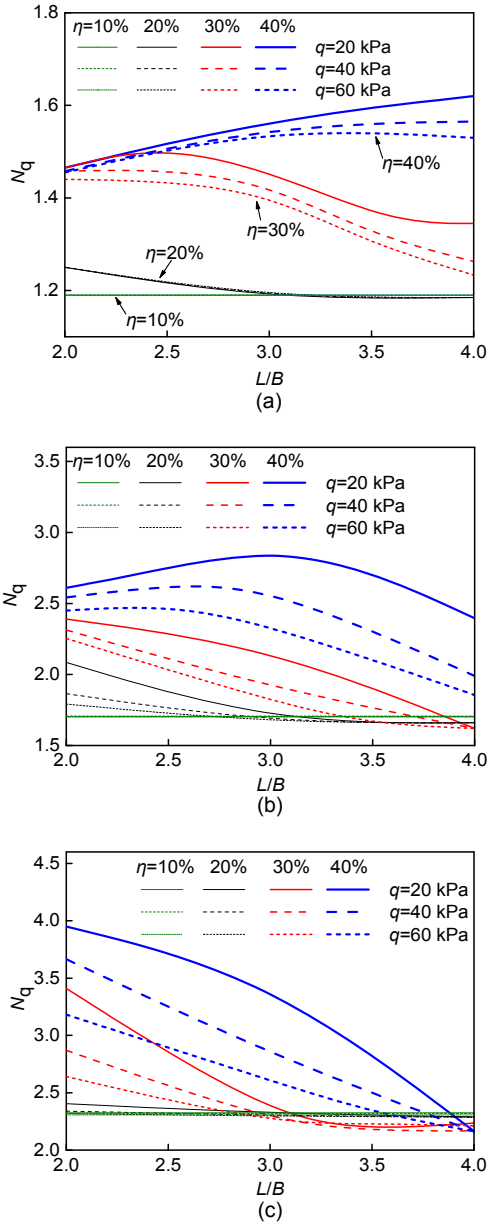

Fig. 8 Bearing capacity charts for coefficient N_q
(a) φ=2°; (b) φ=6°; (c) φ=10°

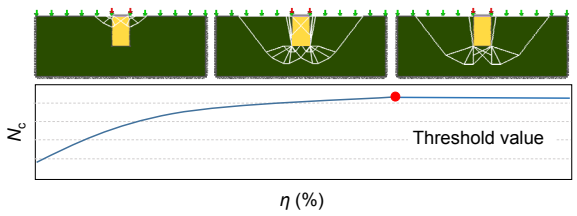

Fig. 9 Schematic of coefficient N_c and the corresponding failure mechanism

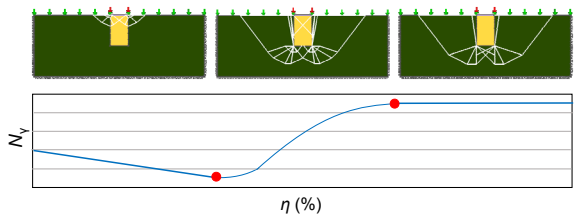

Fig. 10 Schematic of coefficient N_γ and the corresponding failure mechanism

According to the presented design charts of coefficient N_q, three different types of failure patterns

can be identified, as shown in Fig. 11. For the block failure pattern, the N_q value increases with L/B because the increasing column length contributes to greater bearing capacity. However, the N_q value is insensitive to the column length L/B when a failure slip occurs within the reinforced region, and additional column length does not benefit the N_q value. A complex trend of N_q values can be observed in the shift of the failure mechanism. The starting point represents a block failure pattern. The curves show an initial increase of N_q with increasing column lengths due to the deepened surface slip, which leads to larger bearing capacity. As L/B further increases, N_q begins to decrease because of the local shear failure pattern. In this failure type, the contribution of column length on bearing capacity becomes unapparent. With the further increase of column length, the load cannot transfer to the column base and a general shear failure pattern appears, in which the coefficient N_q becomes insensitive to additional column length.

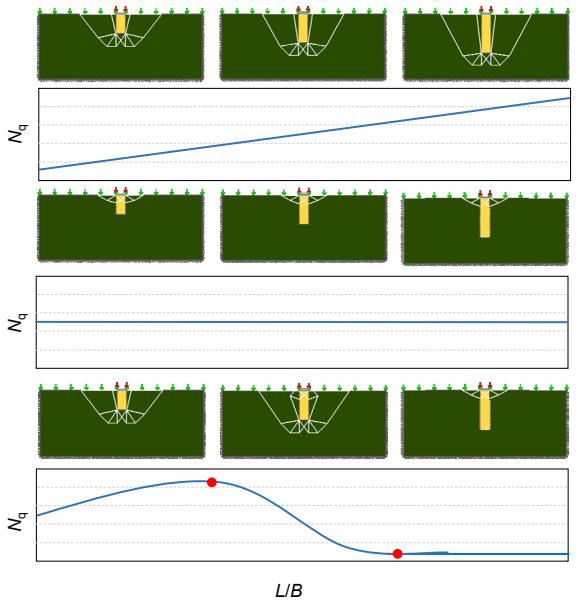

Fig. 11 Schematic of coefficient N_q and the corresponding failure mechanism

5 Conclusions

The results of this investigation were obtained using the DLO technique. The failure mechanism and bearing capacity coefficients of composite ground, which are improved by floating DM columns subjected to varying levels of surcharge, were investigated. The following conclusions can be drawn:

1. DLO is found to be a capable tool for evaluating bearing capacity factors for a group of DM columns. Application of limit analysis combined with the equivalent area model accurately captures the limit loads and failure mechanism through a comparison with the individual column model and the results of previous studies.

2. The bearing capacity factors are found to be governed by the critical failure mechanism that is determined for the ultimate limit load. For reinforced ground without surcharge, a critical value of area replacement ratio for the coefficient N_c represents the shift of the failure mechanism, indicating the highest N_c value. Generally, the coefficient N_γ shows a reduction trend with increasing η because of the decrease of the equivalent frictional strength in the reinforced region.

3. The failure mechanism and corresponding bearing capacity are found to be complex when the surcharge is considered. Specifically, an increasing and constant trend for N_q is observed for the column length under the general shear failure pattern and the block failure pattern, respectively. An increase in column length results in larger N_q until the failure mechanism changes from the block failure pattern to the local shear failure pattern. With further increases in the column length, the N_q value becomes small because the effect of additional column length on the bearing capacity is minimal.

This investigation presents design charts with a reasonable range of parameters but does not account for all scenarios. The developed design charts can be used for preliminary design applications.

References

Aboshi H, Ichimoto E, Enoki M, et al., 1979. The compozer–a method to improve characteristics of soft clays by inclusion of large diameter sand columns. Proceedings of the International Conference on Soil Reinforcement: Reinforced Earth and Other Techniques.

Abusharar SW, Han J, 2011. Two-dimensional deep-seated slope stability analysis of embankments over stone column-improved soft clay. *Engineering Geology*, 120(1-4):103-110. https://doi.org/10.1016/j.enggeo.2011.04.002

Bouassida M, Porbaha A, 2004. Ultimate bearing capacity of soft clays reinforced by a group of columns: application to a deep mixing technique. *Soils and Foundations*, 44(3): 91-101.
https://doi.org/10.3208/sandf.44.3_91

Bouassida M, Jelali B, Porbaha A, 2009. Limit analysis of rigid foundations on floating columns. *International Journal of Geomechanics*, 9(3):89-101.
https://doi.org/10.1061/(ASCE)1532-3641(2009)9:3(89)

Broms BB, 1991. Stabilization of soil with lime columns. *In*: Fang HY (Ed.), Foundation Engineering Handbook. Springer, Boston, USA, p.833-855.
https://doi.org/10.1007/978-1-4757-5271-7_24

Broms BB, 2000. Lime and lime/columns. Summary and visions. Proceedings of the 4th International Conference on Ground Improvement Geosystems, p.43-93.

Bruce DA, 2001a. An Introduction to the Deep Mixing Methods as Used in Geotechnical Applications, Volume III: the Verification and Properties of Treated Ground. Report No. FHWA-RD-99-167, the National Academies of Sciences, Engineering, and Medicine, USA.

Bruce DA, 2001b. Practitioner's guide to the deep mixing method. *Proceedings of the Institution of Civil Engineers–Ground Improvement*, 5(3):95-100.
https://doi.org/10.1680/grim.2001.5.3.95

Cai YQ, Xu CJ, 2002. Consolidation behavior of cement- and lime/cement-mixed column foundations. *Journal of Zhejiang University-SCIENCE*, 3(5):507-512.
https://doi.org/10.1631/jzus.2002.0507

Chai JC, Shrestha S, Hino T, et al., 2015. 2D and 3D analyses of an embankment on clay improved by soil-cement columns. *Computers and Geotechnics*, 68:28-37.
https://doi.org/10.1016/j.compgeo.2015.03.014

Chai JC, Shrestha S, Hino T, et al., 2017. Predicting bending failure of CDM columns under embankment loading. *Computers and Geotechnics*, 91:169-178.
https://doi.org/10.1016/j.compgeo.2017.07.015

Dehghanbanadaki A, Ahmad K, Ali N, 2016. Experimental investigations on ultimate bearing capacity of peat stabilized by a group of soil-cement column: a comparative study. *Acta Geotechnica*, 11(2):295-307.
https://doi.org/10.1007/s11440-014-0328-x

Duan Y, Zhang YP, Chan D, et al., 2012. Theoretical elasto-plastic analysis for foundations with geosynthetic-encased columns. *Journal of Zhejiang University-SCIENCE A (Applied Physics & Engineering)*, 13(7):506-518.
https://doi.org/10.1631/jzus.A1100334

Enoki M, Yagi N, Yatabe R, et al., 1991. Shearing characteristic of composite ground and its application to stability analysis. *In*: Deep Foundation Improvements: Design, Construction, and Testing. ASTM International, USA.
https://doi.org/10.1520/STP25048S

Fattah MY, Shlash KT, Al-Waily MJM, 2011. Stress concentration ratio of model stone columns in soft clays. *Geotechnical Testing Journal*, 34(1):50-60.

Han J, 2015. Principles and Practice of Ground Improvement. John Wiley & Sons, USA.

Hanna AM, Etezad M, Ayadat T, 2013. Mode of failure of a group of stone columns in soft soil. *International Journal of Geomechanics*, 13(1):87-96.
https://doi.org/10.1061/(ASCE)GM.1943-5622.0000175

Horpibulsuk S, Miura N, Koga H, et al., 2004. Analysis of strength development in deep mixing: a field study. *Proceedings of the Institution of Civil Engineers–Ground Improvement*, 8(2):59-68.
https://doi.org/10.1680/grim.2004.8.2.59

Huang J, Han J, 2009. 3D coupled mechanical and hydraulic modeling of a geosynthetic-reinforced deep mixed column-supported embankment. *Geotextiles and Geomembranes*, 27(4):272-280.
https://doi.org/10.1016/j.geotexmem.2009.01.001

Juran I, Guermazi A, 1988. Settlement response of soft soils reinforced by compacted sand columns. *Journal of Geotechnical Engineering*, 114(8):930-943.
https://doi.org/10.1061/(ASCE)0733-9410(1988)114:8(930)

Karstunen M, 1999. Alternative ways of modelling embankments on deep-stabilized soil. Proceedings of the International Conference on Dry Mix Methods for Deep Soil Stabilization, p.221-228.

Kitazume M, Yamamoto M, 1998. Stability of group column type DMM ground. *Report of Port and Harbour Institute*, 37(2):3-28.

Kitazume M, Terashi M, 2002. The Deep Mixing Method–Principle, Design and Construction. Coastal Development Institute of Technology, Japan.

Kitazume M, Yamamoto M, Udaka Y, 1999. Vertical bearing capacity of column type DMM ground with low improvement ratios. Proceedings of the International Conference on Dry Mix Methods for Deep Soil Stabilization, p.245-250.

Kitazume M, Okano K, Miyajima S, 2000. Centrifuge model tests on failure envelope of column type deep mixing method improved ground. *Soils and Foundations*, 40(4): 43-55.
https://doi.org/10.3208/sandf.40.4_43

Leshchinsky B, 2015. Bearing capacity of footings placed adjacent to c'-φ' slopes. *Journal of Geotechnical & Geoenvironmental Engineering*, 141(6):04015022.
https://doi.org/10.1061/(ASCE)GT.1943-5606.0001306

Liu W, Albers B, Zhao Y, et al., 2016. Upper bound analysis for estimation of the influence of seepage on tunnel face stability in layered soils. *Journal of Zhejiang University-SCIENCE A (Applied Physics & Engineering)*, 17(11): 886-902.
https://doi.org/10.1631/jzus.A1500233

Okumura T, 1996. Deep mixing method of Japan. Grouting and deep mixing. Proceedings of the 2nd International

Conference on Ground Improvement Geosystems, p.879-887.

Omine K, Ochiai H, Bolton MD, 1999. Homogenization method for numerical analysis of improved ground with cement treated soil columns. Proceedings of the International Conference on Dry Dry Mix Methods for Deep Soil Stabilization, p.161-168.

Porbaha A, 1998. State of the art in deep mixing technology: part I. Basic concepts and overview. *Proceedings of the Institution of Civil Engineers–Ground Improvement*, 2(2): 81-92.
https://doi.org/10.1680/gi.1998.020204

Porbaha A, Bouassida M, 2004. Bearing capacity of foundations resting on soft ground improved by soil cement columns. International Conference on Geotechnical Engineering, p.172-179.

Priebe HJ, 1995. The design of vibro replacement. *Ground Engineering*, 28(10):31.

Rashid A, Safuan A, 2011. Behavior of Weak Soils Reinforced with Soil Columns Formed by Deep Mixing Method. PhD Thesis, University of Sheffield, UK.

Rashid ASA, Black JA, Kueh ABH, et al., 2015. Behaviour of weak soils reinforced with soil cement columns formed by the deep mixing method: rigid and flexible footings. *Measurement*, 68:262-279.
https://doi.org/10.1016/j.measurement.2015.02.039

Rashid ASA, Black JA, Kueh ABH, et al., 2017. Bearing capacity charts of soft soil reinforced by deep mixing. *Proceedings of the Institution of Civil Engineers–Ground Improvement*, 170(1):12-25.
https://doi.org/10.1680/jgrim.15.00008

Sexton BG, Mccabe BA, Castro J, 2013. Appraising stone column settlement prediction methods using finite element analyses. *Acta Geotechnica*, 9(6):993-1011.
https://doi.org/10.1007/s11440-013-0260-5

Smith C, Gilbert M, 2007. Application of discontinuity layout optimization to plane plasticity problems. *Proceedings of the Royal Society A: Mathematical, Physical and Engineering Sciences*, 463(2086):2461-2484.
https://doi.org/10.1098/rspa.2006.1788

Smith C, Gilbert M, 2013. Identification of rotational failure mechanisms in cohesive media using discontinuity layout optimization. *Geotechnique*, 63(14):1194-1208.
https://doi.org/10.1680/geot.12.P.082

Tan SA, Tjahyono S, Oo KK, 2008. Simplified plane-strain modeling of stone-column reinforced ground. *Journal of Geotechnical and Geoenvironmental Engineering*, 134(2):185-194.
https://doi.org/10.1061/(ASCE)1090-0241(2008)134:2(185)

Tan TS, Goh TL, Yong KY, 2002. Properties of Singapore marine clays improved by cement mixing. *Geotechnical Testing Journal*, 25(4):422-433.
https://doi.org/10.1520/GTJ11295J

Terzaghi K, 1943. Theoretical Soil Mechanics. Wiley, New York, USA.
https://doi.org/10.1002/9780470172766

Wu Y, Diao H, Liu J, et al., 2016. Field studies of a technique to mitigate ground settlement of operating highways. *Journal of Zhejiang University-SCIENCE A (Applied Physics & Engineering)*, 17(7):565-576.
https://doi.org/10.1631/jzus.A1600231

Yapage NNS, Liyanapathirana DS, Kelly RB, et al., 2014. Numerical modeling of an embankment over soft ground improved with deep cement mixed columns: case history. *Journal of Geotechnical and Geoenvironmental Engineering*, 140(11):04014062.
https://doi.org/10.1061/(ASCE)GT.1943-5606.0001165

Ye GB, Zhang Z, Han J, et al., 2013. Performance evaluation of an embankment on soft soil improved by deep mixed columns and prefabricated vertical drains. *Journal of Performance of Constructed Facilities*, 27(5):614-623.
https://doi.org/10.1061/(ASCE)CF.1943-5509.0000369

Yin JH, Fang Z, 2010. Physical modeling of a footing on soft soil ground with deep cement mixed soil columns under vertical loading. *Marine Georesources and Geotechnology*, 28(2):173-188.
https://doi.org/10.1080/10641191003780872

Zhang Z, Han J, Ye G, 2014. Numerical investigation on factors for deep-seated slope stability of stone column-supported embankments over soft clay. *Engineering Geology*, 168(2):104-113.
https://doi.org/10.1016/j.enggeo.2013.11.004

Zheng G, Zhou HZ, Diao Y, et al., 2015. Bearing capacity factor for granular pile composite ground in saturated soft clay. *Chinese Journal of Geotechnical Engineering*, 37(3):385-399 (In Chinese).

Zhou HZ, Diao Y, Zheng G, et al., 2017. Failure modes and bearing capacity of strip footings on soft ground reinforced by floating stone columns. *Acta Geotechnica*, 12(5):1089-1103.
https://doi.org/10.1007/s11440-017-0535-3

Zhou HZ, Zheng G, Yin X, et al., 2018. The bearing capacity and failure mechanism of a vertically loaded strip footing placed on the top of slopes. *Computers and Geotechnics*, 94:12-21.
https://doi.org/10.1016/j.compgeo.2017.08.009

中文概要

题　目：水泥搅拌桩复合地基的承载力与破坏模式研究

目　的：工程规范中采取保守设计方法导致含有埋深的复合地基的承载力被严重低估。本文基于设计表格的方法展示水泥搅拌站复合地基的承载力系数（N_c、N_q和N_γ），分析埋深存在时的3种破坏模式，探讨承载力系数N_q和破坏模式随着各类因素

（桩长、置换率和埋置深度）变化的原因。

创新点： 1. 确定简化的均质化水泥搅拌桩加固地基模型；2. 建立非连续布局优化法（DLO）模型，计算工程实用设计表格；3. 分析极限承载力系数 N_q、破坏模式和各类影响因素的内在关联。

方　法： 1. 通过等效强度法确定合理的均质化数值计算模型，并与群桩模型和前人研究进行对比验证（图 4 和表 1）；2. 通过极限分析上限解结合非连续布局优化法，进行大量计算，建立极限承载力系数的设计表格（图 6~8）。

结　论： 1. 对于无埋深工况，承载力系数 N_c 随着置换率的增长而增大，直到某一临界值，此时发生实体基础破坏。2. 在置换率较低时，承载力系数 N_γ 随着置换率的增长而减小，因为此时加固区内的等效内摩擦角减小。3. 埋置深度对承载力和破坏模式产生复杂影响；当破坏模式从实体基础转化为复合型破坏时，N_q 增长；随着桩长进一步增加，破坏面通过加固区内部时，N_q 在减小之后保持不变。

关键词： 承载力；水泥搅拌桩；埋置深度；破坏模式